International Journal for Uncertainty Quantification, 3 (1): 39–46 (2013)

COMPUTING GREEN'S FUNCTIONS FOR FLOW IN HETEROGENEOUS COMPOSITE MEDIA

David A. Barajas-Solano & Daniel M. Tartakovsky*

Department of Mechanical and Aerospace Engineering, University of California, San Diego, 9500 Gilman Drive, Mail Code 0411, La Jolla, California 92093-0411, USA

Original Manuscript Submitted: 07/06/2011; Final Draft Received: 09/12/2011

Green's functions lie at the foundation of many uncertainty quantification and uncertainty reduction techniques (e.g., the moment differential equation approach, parameter and/or source identification, and data assimilation). We discuss an accurate and numerically efficient approach to compute Green's functions for transport processes in heterogeneous composite media. We focus on elliptic partial differential equations with (random) discontinuous coefficients. The approach relies on a regularization technique to obtain an associated regular problem, which can be solved using standard finite element methods. We perform numerical experiments to assess the performance of the regularization approach and to evaluate the effects of strong coefficient discontinuities on the Green's function behavior.

KEY WORDS: *uncertainty quantification, stochastic elliptical partial differential equations, moment differential equation, composite media*

1. INTRODUCTION

Green's functions are often used to quantify parametric uncertainty in physical systems described by partial differential equations (PDEs). They allow for direct analysis of the effects of uncertain forcings (source functions, initial and boundary conditions) whose effect is additive, and facilitate quantification of uncertainty in system parameters (conductivity, porosity, etc.) whose effect is multiplicative. Green's functions were employed to handle random parameters in a variety of fields, including dispersion of passive scalars in turbulent flows [1], flow and reactive transport [2–8] in porous media, subsurface imaging [9], and parameter estimation and source identification [10].

Our analysis is motivated by the nonlocal formalism [2, 3], which employs moment differential equations (MDEs) to quantify uncertainty in predictions of steady-state flow in heterogeneous porous media with uncertain conductivity. The approach we propose relies on Green's functions to represent the nonlocal nature of the ensemble statistics of a system's response (i.e., hydraulic heads and fluxes). This methodology, coupled with asymptotic expansions in (small) variances of system parameters, was used to model linear [4], nonlinear [11], and free-surface [7, 12] flows, as well as transport of chemically inert [13, 14] and active [8] solutes in porous media with statistically homogeneous and inhomogeneous [6] uncertain (random) parameters.

A typical example of the use of Green's functions in the context of uncertainty quantification is the computation of statistics of the hydraulic head h for steady saturated flow, governed by an elliptic equation [4]

$$\nabla \cdot [k(\mathbf{x})\nabla h(\mathbf{x})] + f(\mathbf{x}) = 0, \qquad \mathbf{x} \in \Omega, \tag{1}$$

where uncertain hydraulic conductivity $k(\mathbf{x})$ and source function $f(\mathbf{x})$ are modeled as random fields. Let $Y(\mathbf{x}) = \ln K(\mathbf{x})$ be multivariate Gaussian, with mean $\langle Y \rangle$ and variance σ_Y^2, and correlation function $C_Y(\mathbf{x}, \mathbf{y})$. For mildly heterogeneous media with small variances σ_Y^2, the mean hydraulic head $\langle h(\mathbf{x}) \rangle$ can be expanded into a perturbation series in powers of σ_Y^2 [4],

$$\langle h(\mathbf{x}) \rangle = \langle h^{(0)}(\mathbf{x}) \rangle + \langle h^{(1)}(\mathbf{x}) \rangle + \dots . \tag{2}$$

*Correspond to Daniel M. Tartakovsky, E-mail: dmt@ucsd.edu

2152–5080/13/$35.00

The zeroth-order approximation satisfies

$$\nabla \cdot [K \nabla \langle h^{(0)}(\mathbf{x}) \rangle] + \langle f(\mathbf{x}) \rangle = 0, \tag{3}$$

where K is the geometric mean of the field $k(\mathbf{x})$. The first-order approximation can then be computed as

$$\langle h^{(1)}(\mathbf{x}) \rangle = -\int_\Omega \left[K \frac{\sigma_Y^2}{2} \nabla_{\mathbf{y}} \langle h^{(0)}(\mathbf{y}) \rangle - \hat{\mathbf{r}}^{(1)}(\mathbf{y}) \right] \cdot \nabla_{\mathbf{y}} G(\mathbf{y}; \mathbf{x}) \, d\mathbf{y}. \tag{4}$$

In this expression, $G(\mathbf{y}; \mathbf{x})$ is the Green's function associated with (3) and $\hat{\mathbf{r}}^{(1)}(\mathbf{x})$ is given by

$$\hat{\mathbf{r}}^{(1)}(\mathbf{y}) = K^2 \int_\Omega C_Y(\mathbf{x}, \mathbf{y}) \nabla_{\mathbf{y}} \nabla_{\mathbf{x}}^\top G(\mathbf{y}; \mathbf{x}) \nabla_{\mathbf{y}} \langle h^{(0)}(\mathbf{y}) \rangle \, d\mathbf{y}. \tag{5}$$

Other statistics of $h(\mathbf{x})$ can be expressed in terms of the Green's function G as well.

When Green's functions are derived analytically, such approaches can be computationally more efficient than Monte Carlo simulations and other numerical techniques for solving stochastic PDEs. They also provide physical insight into how uncertainty in parameters and/or driving forces affects predictive uncertainty. However, Green's functions for many problems of practical significance cannot be obtained analytically. The need to compute Green's functions numerically is by far the largest computational expense in the uncertainty quantification approaches that rely on them.

The presence of the Dirac delta function in a Green's function PDE compromises the accuracy and convergence of regular finite element methods [15]. Further contributing to the loss of solution regularity are discontinuous coefficients in the governing PDEs [16] that describe, for example, flow in heterogeneous composite media [6]. The ability to compute Green's functions efficiently in such a setting is of crucial importance to many uncertainty quantification efforts. Meeting this goal for uncertainty quantifications in elliptic PDEs is the major goal of the present analysis.

Green's functions of some elliptic operators decay with the distance from the location of the Dirac forcing (point source). It is therefore possible to speak of a "support domain" for the Green's function, defined as a portion of the computational domain in which the function is nonzero with a given degree of accuracy. Outside of the support domain the Green's function is small enough not to affect a global quantity, e.g., an integral or another quantity dependent on the function in a weak sense. In such a case, homogeneous boundary conditions of a Green's function PDE are transferred to the boundary of the support domain. Being able to solve a Green's function PDE on the support domain, a (small) subset of the computational domain, leads to a significant reduction in computational time.

2. REGULARIZED FORMULATION OF GREEN'S FUNCTION PROBLEM

Let $\Omega \subset \mathbb{R}^d$ ($d = 1, 2, 3$) denote a convex domain with the Lipschitz-continuous boundary Γ. The domain Ω is composed of two disjoint units Ω_1 and Ω_2 such that $\Omega = \Omega_1 \cup \Omega_2$ with Γ_{12} being the boundary between them (Fig. 1). Consider an elliptic PDE for the Green's function $G(\mathbf{x}; \mathbf{x}_0)$,

$$-\nabla \cdot [K(\mathbf{x}) \nabla G(\mathbf{x}; \mathbf{x}_0)] = \delta(\mathbf{x} - \mathbf{x}_0) \qquad \text{in} \qquad \mathbf{x}, \mathbf{x}_0 \in \Omega, \tag{6}$$

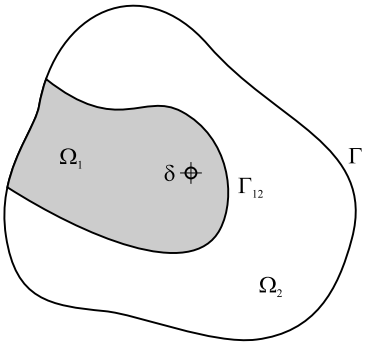

FIG. 1: Composite domain Ω.

subject to the boundary conditions

$$G(\mathbf{x}) = 0 \quad \text{on} \quad \mathbf{x} \in \Gamma_D \tag{7}$$

$$\nabla G(\mathbf{x}) \cdot \mathbf{n} = 0 \quad \text{on} \quad \mathbf{x} \in \Gamma_N. \tag{8}$$

The coefficient $K(\mathbf{x})$ is piecewise constant in Ω_1 and Ω_2, $\delta(\mathbf{x} - \mathbf{x}_0)$ is the Dirac delta function centered at point $\mathbf{x}_0$, and $\mathbf{n}$ is the unit normal vector pointing outward of Ω. The Dirichlet and Neumann boundary conditions are prescribed in the boundary segments Γ_D and Γ_N ($\Gamma = \Gamma_D \cap \Gamma_N$), respectively. Along the interface Γ_{12}, the Green's function and its flux satisfy the continuity conditions

$$[G(\mathbf{x})]_{\Gamma_{12}} = 0, \quad [K\nabla G(\mathbf{x}) \cdot \mathbf{n}_{12}]_{\Gamma_{12}} = 0, \tag{9}$$

where $[\cdot]$ denotes the jump of an enclosed quantity across the interface, and $\mathbf{n}_{12}$ is the unit vector normal to Γ_{12}, pointing from Ω_1 to Ω_2. The Green's function G is singular at $\mathbf{x} = \mathbf{x}_0$ due to the Dirac forcing.

Let $H^1(\Omega)$ be the space of square-integrable functions with square-integrable weak derivatives up to the first order, and V its subspace given by

$$V = \{v \in H^1(\Omega) : v|_{\Gamma_D} = 0\}. \tag{10}$$

Multiplying both sides of (6) with $v \in V$ and applying the Green's theorem, one obtains the following weak formulation: Find $G_d \in V$ such that

$$\int_\Omega K(\mathbf{x}) \nabla G_d \cdot \nabla v \, d\mathbf{x} = v(\mathbf{x}) \quad \text{for all} \quad v \in V. \tag{11}$$

The problem with this standard formulation is that $G \notin H^1(\Omega)$ due to the singularity at $\mathbf{x}_0$. This implies that the solution G of (6) is not globally smooth enough for G_d to converge to G in the limit of mesh refinement [15]. In order to overcome this issue, we follow the finite element strategy [15–17] for solving the Poisson-Boltzmann equation (6). The approach divides the solution into a singular part and a regular part [17]. The regular problem admits an unique solution $\tilde{G} \in H^1$ and thus can be computed using a standard finite element approach [16].

To illustrate the regularization methodology, consider a domain Ω such that the boundary Γ_1 of Ω_1 contains a portion of the domain boundary Γ, and let $\mathbf{x}_0 \in \Omega_1$. Following [16], the total solution G can be decomposed into three components G_s, G_h, and $\tilde{G}$ such that

$$G = \begin{cases} G_s + G_h + \tilde{G} & \text{if } \mathbf{x} \in \Omega_1, \\ \tilde{G} & \text{if } \mathbf{x} \in \Omega_2. \end{cases} \tag{12}$$

We define G_s, the *singular* component, as a solution of

$$-\nabla \cdot (K_1 \nabla G_s) = \delta(\mathbf{x} - \mathbf{x}_0), \quad \mathbf{x} \in \mathbb{R}^d. \tag{13}$$

That is, G_s is the free-space Green's function for Laplace's equation with forcing δ/K_1. For $d = 2$, $G_s = -(2\pi K_1)^{-1} \ln(|\mathbf{x} - \mathbf{x}_0|)$ where $|\cdot|$ is the Euclidean norm. We also define the component G_h, the harmonic extension of the trace of the singular component G_s on Γ_1 into Ω_1, as a solution of

$$-\nabla \cdot (K_1 \nabla G_h) = 0 \quad \text{in} \quad \mathbf{x} \in \Omega_1, \quad G_s + G_h = 0 \quad \text{on} \quad \mathbf{x} \in \Gamma_1. \tag{14}$$

Substituting (12)–(14) into (6) and enforcing the boundary conditions (7) and (8), one obtains the following problem for the *regular* component $\tilde{G}$:

$$\begin{aligned} -\nabla \cdot (K(\mathbf{x}) \nabla \tilde{G}) &= 0 \quad \text{in} \quad \mathbf{x} \in \Omega, \\ \tilde{G} &= 0 \quad \text{on} \quad \mathbf{x} \in \Gamma_D, \\ \nabla(\tilde{G} + G_s + G_h) \cdot \mathbf{n} &= 0 \quad \text{on} \quad \mathbf{x} \in \Gamma_N, \\ [\tilde{G}] &= 0 \quad \text{on} \quad \mathbf{x} \in \Gamma_{12}, \\ [K(\mathbf{x}) \nabla \tilde{G} \cdot \mathbf{n}_{12}] &= K_1 \nabla (G_s + G_h) \cdot \mathbf{n}_{12} \quad \text{on} \quad \mathbf{x} \in \Gamma_{12}. \end{aligned} \tag{15}$$

It is proved in [16] that $\tilde{G}$ is unique and lies in $H^1(\Omega)$, thus completing a methodology for approximating numerically the solution of (6).

2.1 Extensions of the Regularization Formulation

The approach described above can be generalized to more elaborate Green's function problems as long as a singular component analogous to (13) can be computed in closed form. Consider for example the equation

$$-\nabla \cdot [K(\mathbf{x})\nabla G] + \alpha \frac{\partial}{\partial x_3}[K(\mathbf{x})G] = \delta(\mathbf{x} - \mathbf{x}_0), \tag{16}$$

which arises in the context of unsaturated flow in porous media [5]. For constant $K = K_1$, the free-space solution of this problem is

$$G_s = -\frac{1}{2\pi K_1} \mathrm{e}^{-\alpha(x_3 - x_{0,3})/2} \mathcal{K}_0(\alpha|\mathbf{x} - \mathbf{x}_0|/2),$$

where $\mathcal{K}_0$ is the zeroth-order modified Bessel function of the second kind. A harmonic expansion and a regular component can be defined in a fashion similar to (14) and (15).

Another possible generalization is the relaxation of the piecewise constant condition on $K(\mathbf{x})$ to the weaker piecewise Lipschitz continuity [18]. Such $K(\mathbf{x})$ fields capture small-scale variability inside each domain Ω_i, superimposed on large-scale variability between domains. Consider a setting similar to (6), but with the piecewise Lipschitz continuous $K(\mathbf{x})$. While K_1 is no longer constant, we nevertheless define the singular component G_s as a solution of

$$-\nabla \cdot (K^* \nabla G_s) = \delta(\mathbf{x} - \mathbf{x}_0), \quad \mathbf{x} \in \mathbb{R}^d, \tag{17}$$

where $K^* = K(\mathbf{x}_0)$. This solution is often available analytically, and from it one can define the harmonic extension in a weak sense as a solution $G_h \in V_1$ of

$$\int_{\Omega_1} K(\mathbf{x}) \nabla G_h \cdot \nabla v \, d\mathbf{x} = \int_{\Omega_1} [K^* - K(\mathbf{x})] \nabla G_s \cdot \nabla v \, d\mathbf{x} \quad \text{for all} \quad v \in V_1, \tag{18}$$

with $V_1 = \{v \in H^1(\Omega) : v|_{\Gamma_1} = 0\}$. The remaining regular component is defined in a manner analogous to (15).

3. NUMERICAL EXAMPLES

The regularized formulation of the Green's function problem discussed in the previous section makes it explicit that differing values of K within subdomains Ω_i ($i = 1, 2$) affect the global behavior of the Green's function. This difference can be of one order of magnitude as in the Poisson-Boltzmann problem, or of many orders of magnitude as in subsurface applications [19]. To study the effect this difference has on a solution of the Green's function, we solve (6) on the domain shown in Fig. 2, with $K_1 = 1.0$ and $K_2 = 10.0$ or 0.1. The solutions G for both cases, computed using linear triangular finite elements and a grid size $h = 0.02$, are shown in Fig. 3.

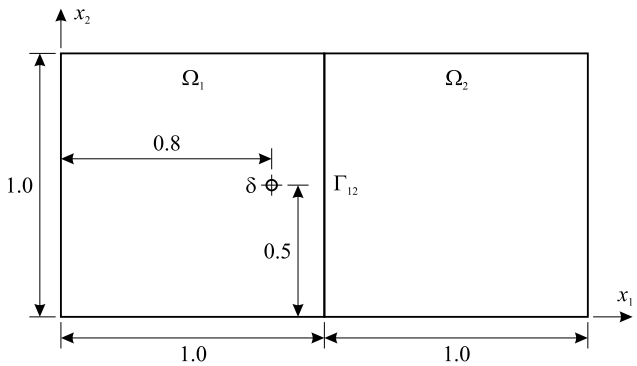

FIG. 2: Domain of example 1.

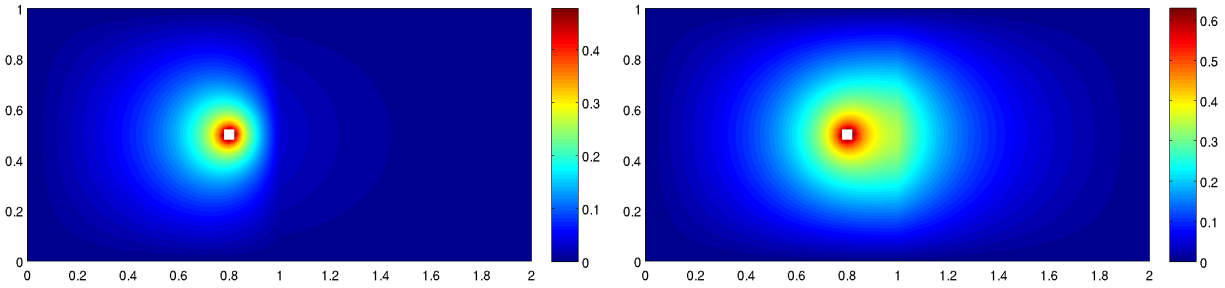

(a) (b)

FIG. 3: Green's functions of example 1 with $K_1 = 1$ and (a) $K_2 = 10$, (b) $K_2 = 0.1$.

To assess the accuracy of the regularization approach compared to a standard discrete approximation, we computed solutions to the previous problem, using both the regularization approach and the discrete approximation G_d of (11), for different grid sizes h. For each value of h, let $\mathcal{E}_p$ and $\mathcal{E}_h$ denote the absolute difference between G and G_d at point $(0.5, 0.5)$ and at a distance h in the x_1 direction from the point source, respectively. Table 1 shows that $\mathcal{E}_p$ decays with h as h^2, while $\mathcal{E}_h$ remains constant independent of grid size; this confirms that G_d does not converge uniformly to G in the limit of mesh refinement, as stated in [15]. This result is to be expected as it is not possible for an approximation in H^1 to capture the behavior of the Green's function in the vicinity of the singularity. The regularization approach is more accurate than the standard discrete approximation, especially for low-resolution (large grid size h) simulations in which the vicinity of the singularity can be rather large.

Next we evaluate the size of the support domains of the Green's functions in Fig. 3. Figure 3(a) shows that if the Dirac impulse is located in the low-K region, then the support domain lies within Ω_1 and a portion of Ω_2 in the vicinity of Γ_{12}. If the Dirac impulse lies within the high-K region, then the jump conditions (9) at the interface Γ_{12} can be approximated with the homogeneous Neumann (no-flow) boundary condition for the Green's function PDE defined on Ω_1 and the Green's function PDE defined on Ω_2 is subject to the continuity (Dirichlet) condition $[G] = 0$ for $\mathbf{y} \in \Gamma_{12}$. The two PDEs become decoupled, and the support domain of G becomes larger [Fig. 3(b)].

To illustrate these points further, we compute solutions of (6) defined on the $L \times L$ square domain shown in Fig. 4. Its internal geometry is reconstructed in [19] from synthetic geostatistical data by means of indicator kriging with $K_1 = \exp(-0.1)$ and $K_2 = \exp(7.0)$. The Green's function, for the Dirac forcing placed in both subdomains, is presented in Fig. 5.

As expected from the earlier discussion, Fig. 5(a) shows that the Green's function with $\mathbf{x}_0$ in the low-K region has the support domain restricted to that subdomain. A sizable portion of the rest of the domain can then be disregarded, with the extent of that reduction depending on the level of accuracy required. The Dirac forcing located in the high-K region significantly extends the support domain, reducing the aforementioned numerical advantages.

Finally, we use the Green's functions in Fig. 5 to solve a stochastic problem

$$\nabla \cdot [K(\mathbf{x})\nabla h(\mathbf{x})] + f(\mathbf{x}) = 0, \qquad \mathbf{x} \in \Omega, \tag{19}$$

TABLE 1: Absolute differences $\mathcal{E}_p$ and $\mathcal{E}_h$ for various grid sizes

h	$\mathcal{E}_p$		$\mathcal{E}_h$	
	$K_1 = 1, K_2 = 10$	$K_1 = 1, K_2 = 0.1$	$K_1 = 1, K_2 = 10$	$K_1 = 1, K_2 = 0.1$
0.02	5.98×10^{-5}	4.58×10^{-5}	7.3×10^{-3}	7.3×10^{-3}
0.025	9.39×10^{-5}	7.17×10^{-5}	7.3×10^{-3}	7.3×10^{-3}
0.05	3.96×10^{-4}	3.02×10^{-4}	7.3×10^{-3}	7.1×10^{-3}
0.10	1.89×10^{-3}	1.44×10^{-3}	7.3×10^{-3}	7.7×10^{-3}

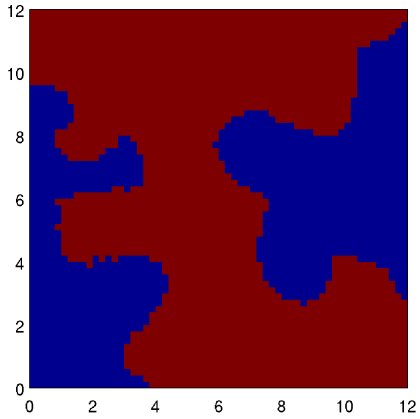

FIG. 4: Domain of example 2. K_1 (blue) $= \exp(-0.1)$, K_2 (red) $= \exp(7.0)$, $L = 12$.

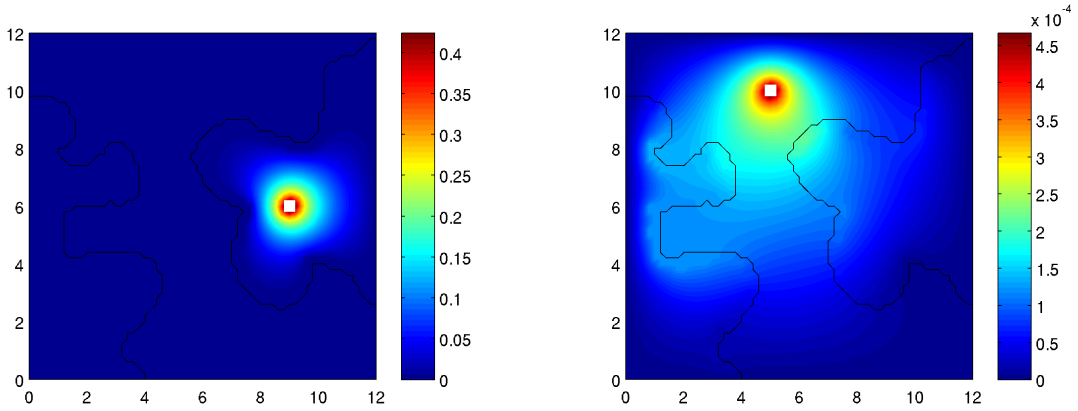

(a) (b)

FIG. 5: Green's functions of example 2 for (a) $\mathbf{x}_0 = (9, 6)$, (b) $\mathbf{x} = (5, 10)$.

in the composite domain Ω of Fig. 4 subjected to homogeneous Dirichlet boundary conditions. The source function $f(\mathbf{x})$ is a stationary random field with unit mean and variance, and exponential correlation function $C_f(\mathbf{x}, \mathbf{y}) = \exp(-|\mathbf{x} - \mathbf{y}|/l)$ with correlation length $l = L/2$. In terms of the Green's function for problem (6), the mean and variance of h can be written as

$$\langle h(\mathbf{x}) \rangle = \int_\Omega \langle f(\mathbf{y}) \rangle G(\mathbf{y}; \mathbf{x})\, d\mathbf{y}, \tag{20}$$

$$\sigma_h^2(\mathbf{x}) = \iint_{\Omega\times\Omega} C_f(\mathbf{y}, \mathbf{z}) G(\mathbf{y}; \mathbf{x}) G(\mathbf{z}; \mathbf{x})\, d\mathbf{y} d\mathbf{z}. \tag{21}$$

Results computed using (20) and (21) are shown in Fig. 6.

4. CONCLUSIONS

A regularization methodology for the numerical computation of Green's functions of elliptic boundary value problems in heterogeneous composite media has been studied. Green's functions are routinely used in uncertainty quantification, particularly in the moment differential equations approach to solving stochastic partial differential equations. Numerical experiments confirm that the regularization methodology allows for accurate and computationally efficient

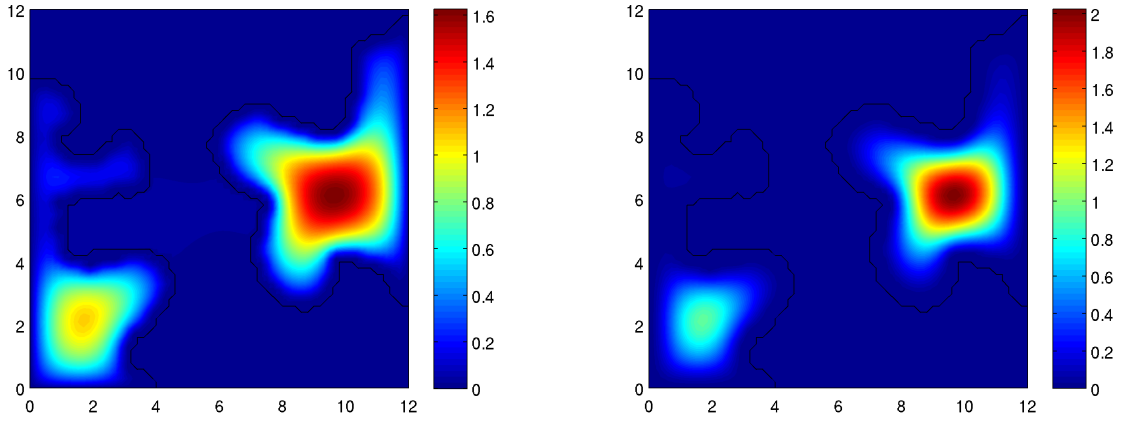

(a) (b)

FIG. 6: Mean (a) and variance (b) of hydraulic conductivity of example 3.

computation of Green's functions compared to standard methods that do not take into account the lack of regularity of the solution stemming from the Dirac forcing. In the case of composite media with discontinuous coefficients, the strength of the jump and the location of the forcing have a damping or amplifying effect on the value of the Green's function throughout the domain. If damping occurs, the opportunity arises for reducing the support domain of the Green's function, thus reducing the problem size and cutting the computation cost.

ACKNOWLEDGMENTS

This research was supported by the DOE Office of Science Advanced Scientific Computing Research (ASCR) program in Applied Mathematical Sciences; and by research grant no. IS-4090-08R from BARD, the United States—Israel Binational Agricultural Research and Development Fund.

REFERENCES

1. Kraichnan, R. H., Eddy viscosity and diffusivity: Exact formulas and approximations, *Complex Systems*, 1:805–820, 1987.
2. Neuman, S. P. and Orr, S., Prediction of steady state flow in nonuniform geologic media by conditional moments: Exact nonlocal formalism, effective conductivities, and weak approximation, *Water Resour. Res.*, 29:341–364, 1993.
3. Neuman, S. P., Tartakovsky, D. M., Wallstrom, T. C., and Winter, C. L., Correction to the Neuman and Orr Nonlocal theory of steady state flow in randomly heterogeneous media, *Water Resour. Res.*, 32(5):1479–1480, 1996.
4. Tartakovsky, D. M. and Neuman, S. P., Transient flow in bounded randomly heterogeneous domains 1. Exact conditional moment equations and recursive approximations, *Water Resour. Res.*, 34(1):1–12, 1998.
5. Tartakovsky, D. M., Neuman, S. P., and Lu, Z., Conditional stochastic averaging of steady state unsaturated flow by means of Kirchhoff transformation, *Water Resour. Res.*, 35(3):731–745, 1999.
6. Winter, C. L. and Tartakovsky, D. M., Groundwater flow in heterogeneous composite aquifers, *Water Resour. Res.*, 38(8):11, 2002.
7. Tartakovsky, A. M., Neuman, S. P., and Lenhard, R. J., Immiscible front evolution in randomly heterogeneous porous media, *Phys. Fluids*, 15(11):3331–3341, 2003.
8. Tartakovsky, D. M. and Broyda, S., PDF equations for advective-reactive transport in heterogeneous porous media with uncertain properties, *J. Contam. Hydrol.*, 120-121:129–140, 2011.
9. Borcea, L., Papanicolaou, G., Tsogka, C., and Berryman, J., Imaging and time reversal in random media, *Inverse Problems*, 18(5):1247, 2002.

10. Huang, C., Hsing, T., Cressie, N., Ganguly, A. R., Protopopescu, V. A., and Rao, N. S., Bayesian source detection and parameter estimation of a plume model based on sensor network measurements, *Appl. Stoch. Models Bus. Industry*, 26(4):331–348, 2010.
11. Tartakovsky, D. M., Guadagnini, A., and Riva, M., Stochastic averaging of nonlinear flows in heterogeneous porous media, *J. Fluid Mech.*, 492:47–62, 2003.
12. Tartakovsky, A. M., Meakin, P., and Huang, H., Stochastic analysis of immiscible displacement of the fluids with arbitrary viscosities and its dependence on support scale of hydrological data, *Adv. Water Resour.*, 27(12):1151–1166, 2004.
13. Dagan, G., Theory of solute transport by groundwater, *Ann. Rev. Fluid Mech.*, 19:183–215, 1987.
14. Morales-Casique, E., Neuman, S. P., and Guadagnini, A., Nonlocal and localized analyses of nonreactive solute transport in bounded randomly heterogeneous porous media: Theoretical framework, *Adv. Water Resour.*, 29(8):1238–1255, 2006.
15. Chen, L., Holst, M. J., and Xu, J., The finite element approximation of the nonlinear Poisson-Boltzmann equation, *SIAM J. Num. Anal.*, 45(6):2298–2320, 2007.
16. Holst, M., McCammon, J. A., Yu, Z., Zhou, Y., and Zhu, Y., Adaptive finite element modeling techniques for the Poisson-Boltzmann equation, *Comm. Comput. Phys.*, 11(1):179–214, 2012.
17. Chern, I.-L., Liu, J.-G., and Wang, W.-C., Accurate evaluation of electrostatics for macromolecules in solution, *Methods Appl. Anal.*, 10(2):309–327, 2003.
18. Chen, Z. and Yue, X., Numerical homogenization of well singularities in the flow transport through heterogeneous porous media, *Multiscale Model. Sim.*, 1(2):260–303, 2003.
19. Wohlberg, B. E., Tartakovsky, D. M., and Guadagnini, A., Subsurface characterization with support vector machines, *IEEE Trans. Geosci. Remote Sens.*, 44(1):47–57, 2006.